

## Thermionic Emission from a Planar Tantalum Crystal\*

HAYWOOD SHELTON†

Department of Physics and Research Laboratory of Electronics, Massachusetts Institute of Technology, Cambridge, Massachusetts

(Received June 4, 1957)

In this investigation two (211) crystals in tantalum ribbon are used as emitter and collector in a three-element retarding-potential experiment. The electrons from one crystal are accelerated through a small aperture which, in conjunction with a strong axial magnetic field, collimates a beam and directs it to the collector crystal. The uniform work-function of single crystals, plane geometry, and the collimating magnetic field completely remove the deleterious effects of conventional retarding-potential experiments that prevent the exact determination of the energy distribution. The resulting retarding-potential plot indicates close agreement with the theoretically predicted two intersecting straight lines on semilogarithmic paper, with the transition region extending less than 20 mv. This indicates a Maxwellian distribu-

tion with no large energy-dependent reflection. A slowly varying 6% reflection, as predicted by quantum mechanics, is observed. The temperature, the saturated current density, and the temperature derivative of the work-function, as found from different retarding-potential plots, are used in a Richardson analysis to derive the thermionic constants. For the clean (211) tantalum surface that was used, the work-function, which is practically temperature-independent, is  $4.352 \pm 0.01$  volts, and the emission constant  $A$  is  $120 \text{ amp/cm}^2 \text{ }^\circ\text{K}^2$ . For differing surfaces resulting from stable layers of foreign adsorbed atoms, the  $A$ , as calculated from a Richardson plot, was demonstrated to differ from 120 solely because of the temperature variation of the work-function.

### I. INTRODUCTION

WHEN statistical mechanics and quantum conditions are applied to free electrons, the Fermi-Dirac distribution results. If the particle current that is derived from this distribution is used to calculate the thermionic current delivered over a barrier  $V$  volts above the Fermi level, the Richardson equation,  $J = 4\pi emk^2 T^2 / h^3 \exp(-eV/kT)$ , is obtained. With the constants evaluated, this equation is written more simply as  $J = AT^2 10^{-5040V/T}$ , where  $A$  is  $120.4 \text{ amp/cm}^2 \text{ }^\circ\text{K}$ .  $V$  (in volts) is the actual barrier measured from the Fermi level, over which an electron must go to be measured as electron current; it equals  $\phi + \Delta V$  when a retarding potential of  $\Delta V$  is added to the work-function  $\phi$  of the emitter. In this case if

$$J_s = AT^2 10^{-5040\phi/T}, \quad (1)$$

$$J = J_s 10^{-5040\Delta V/T}, \quad (2)$$

where  $J_s$  is the saturated current density, collected with an accelerating potential. Equations (1) and (2) are simplified and ideal. There are many known factors, such as space charge, Schottky effect, nonuniform  $\phi$ ,  $d\phi/dT$ , geometry, reflection, and so forth, that prevent the experimentally measured current density from obeying these equations. Because of the large number of these factors, their exact role in explaining the deviation between experiment and theory is vague, especially when the degree and the presence of these factors are uncertain.

The experimental temperature dependence of  $J_s$  is quite satisfactorily given by Eq. (1). However, the two

thermionic constants, as determined from a Richardson plot, although they have been widely tabulated for many materials and are useful in allowing a user to calculate the current he might expect for a given temperature, are not particularly meaningful. The constant  $A$  often differs from 120 by an order of magnitude, and the value of  $\phi$  is not the true work-function. One consideration that is always present is the inherent temperature derivative of the emitter work-function. If  $\phi = \phi_0 + \alpha T$  is inserted in Eq. (1), we observe that the exponential term containing  $\alpha$  is just a constant, so that the experimental value of  $A$  should contain the factor  $10^{-5040\alpha}$ . The experimentally observed  $\phi$  is therefore  $\phi_0$ , the work-function extrapolated to zero temperature, or  $\alpha T$  volts different from the actual work-function. Also, most pure-metal emitters do not have a uniform work-function, since they are polycrystalline and the various exposed crystal faces have different work-functions. Because of the strong dependence of the current density upon the work-function, the measured composite current will come largely from the lower work-function areas, and since the constant  $A$  is calculated by using the entire area, it will be low. The experimental value of  $\phi$  will be some kind of average that is dependent on the patch distribution and the applied field. These points are discussed in detail by Nottingham.<sup>1</sup>

The deficiency of slow electrons in the energy distribution, as found earlier in this laboratory by Nottingham<sup>1</sup> and by Hutson,<sup>2</sup> results in a loss of nearly 50% and would limit the experimental  $A$  to much less than 120, even in the absence of the above-mentioned factors. The deficiency is quantitatively described as a reflection equal to  $\exp(-V/0.191)$ , where  $V$  (in volts) is the energy of the electrons in excess of that needed to escape. This strong energy dependence (100% loss of electrons

\* This work, which was supported in part by the U. S. Army (Signal Corps), the U. S. Navy (Office of Naval Research), and the U. S. Air Force (Office of Scientific Research, Air Research and Development Command), is based on a thesis submitted to the Department of Physics, Massachusetts Institute of Technology, May, 1956, in partial fulfillment of the requirements for the degree of Doctor of Philosophy.

† Now at Ramo-Wooldridge Corporation, Los Angeles, California.

<sup>1</sup> W. B. Nottingham, *Handbuch der Physik* (Springer-Verlag, Berlin, 1956), Vol. 21, pp. 16, 99.

<sup>2</sup> A. R. Hutson, *Phys. Rev.* **98**, 889 (1955).

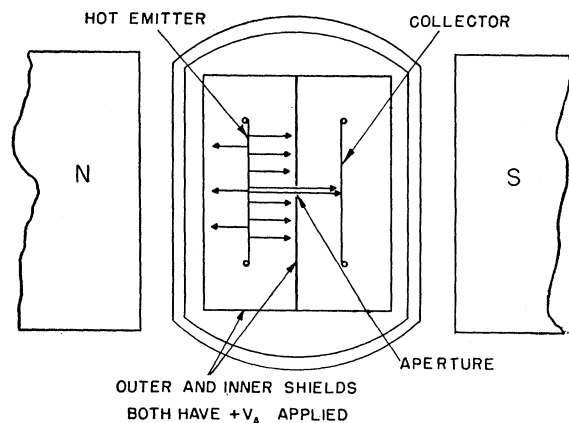


FIG. 1. Schematic of the experimental tube, illustrating how the magnetic field and the single aperture collimate the electrons, thereby defining the emitting area of the sampled current.

with energy just sufficient to escape, decreasing to 37% loss at 0.191 volt) results also in a non-Maxwellian energy distribution. This would produce a retarding-potential plot that would not show  $\log J$  linearly increasing with  $\Delta V$  and then abruptly saturating, as indicated in Eq. (2), but would show  $\log J$  having a gradual transition. Again, there are many other factors that cause gradual transitions in retarding-potential plots: nonuniform work-function on either emitter or collector, geometry, space charge, and field-dependent trajectories. This experiment is able to use the retarding-potential plot to confirm the ideal Maxwellian distribution and deny the  $\exp(V/0.191)$  reflection by eliminating these factors. Single crystals assure a uniform work-function; plane-parallel geometry removes the need for the corrections that are necessary in cylindrical geometry; a third positive intervening electrode reduces space charge and keeps the field at the emitter constant; and a strong axial magnetic field allows the simple design, and also fixes the trajectories and conserves tangential components of the emission. Also,  $d\phi/dT$  can be measured by observing the change in contact potential as the current density and temperature are being measured, so that the meaningful true constants can be calculated from a Richardson analysis.

## II. DESCRIPTION OF THE EXPERIMENT

The distinctive feature of this experiment is that it allows the available form of the crystals to be incorporated simply into an ideal retarding-potential experiment. Although great care was exercised in obtaining the single crystals used in this experiment, small crystals that are quite adequate for general work-function measurements or demonstration purposes are readily grown in tantalum ribbon by heating to above 2500°K in a vacuum for an hour or more. Figure 1 illustrates an experiment in which two of these small crystals can be mounted, directly heated, and used in a retarding-potential experiment, uninfluenced by the

foreign surrounding crystals and the voltage drop in the ribbon. Two ribbons containing single crystals in their centers are mounted face to face. Each ribbon is spot-welded to two parallel tungsten rods, which provide a convenient, rigid mounting, the necessary tension to keep the ribbons taut, and the electric conductance for heating. The collimation that is necessary to insure that all of the sampled current that is collected on the collector crystal originates from a known area of the emitter crystal is accomplished by the strong axial magnetic field and the single aperture. The aperture is in a positive shield between the two ribbons; a positive voltage on the shield accelerates electrons from the emitter. The strong magnetic field will constrain the electrons to move in tight spirals parallel to the magnetic field. Addition of energy to the electrons in a direction perpendicular to the field will result in circular motion with no net drift in that plane. The positive aperture and the emitter, in conjunction with the magnetic field, form a gun that directs a beam of electrons originating from the emitter crystal toward the collector crystal. The cross section of the beam is just that of the aperture, which has a known area for determining the current density. This area is small, so that it is included completely by each crystal, and the  $IR$  drop when the ribbon is directly heated is negligible.

The pencil of electrons can then be analyzed by recording the collected current as a function of the retarding potential applied between the emitter and the collector. From a plot of this current, we can determine the temperature, the amount of reflection, the saturated current density, and the contact potential (the difference in work-function measured by that potential which must be applied to make the retarding potential just equal to zero).

The crystal direction used was the (211), since that direction is the one that almost always results. A lower work-function surface was desired, but none was ever found. Both crystals used were cut from the same single crystal, which was judged to be as perfect as possible by back-reflection Laue x-ray pictures and microscopic examination. The crystals were spot-welded into the centers of 0.003-inch by 0.042-inch by 0.75-inch ribbons. These ribbons had 1-mil tantalum potential leads spot-welded equidistantly from either side of the centers for monitoring the potential drop with a type *K* potentiometer. (The voltage drop during operation was about 1 volt per inch; the current was about 6 amp.) The aperture was a rectangle, approximately 0.007 inch by 0.024 inch, placed midway between the two ribbons at a distance of 0.3 inch from each. The ribbons and aperture were enclosed for shielding, with provision for viewing the ribbons for pyrometric confirmation of the temperature. The elements were mounted in a flattened portion of a Pyrex tube which could be placed between the jaws of a 3000-gauss permanent magnet. The experimental tube, a getter tube, and a Bayard-Alpert ionization gauge were thoroughly baked, processed,

and sealed off. Evaporated molybdenum and tungsten were the gettering agents. During the course of the experiment the total pressure (mostly helium) in the tube was approximately  $1 \times 10^{-10}$  mm Hg, nitrogen equivalent. The pressure of adsorbable gases was lower than  $1 \times 10^{-12}$  mm Hg, as judged by adsorption rates.

Current for heating the filament was obtained from a 6-volt storage battery and an electronic regulator that monitored the total emission current. The constancy of this regulated heating current could be monitored with a type *K* potentiometer across the potential leads. The collector current was measured by a vacuum-tube microammeter, which was maintained calibrated to a few tenths of 1%. The retarding potential obtained directly from a type *K* potentiometer was applied between the collector and the appropriate spot of an external voltage divider across the emitter potential leads. The small drop across the microammeter was taken into account.

III. DISCUSSION OF RESULTS

If the theory outlined in Eq. (1) and Eq. (2) is correct and if all of the usual disturbing factors are eliminated in the design, the resulting retarding-potential current should have the same exponential dependence on the voltage characteristic of the temperature extending to the point of saturation. In Fig. 2 the resulting

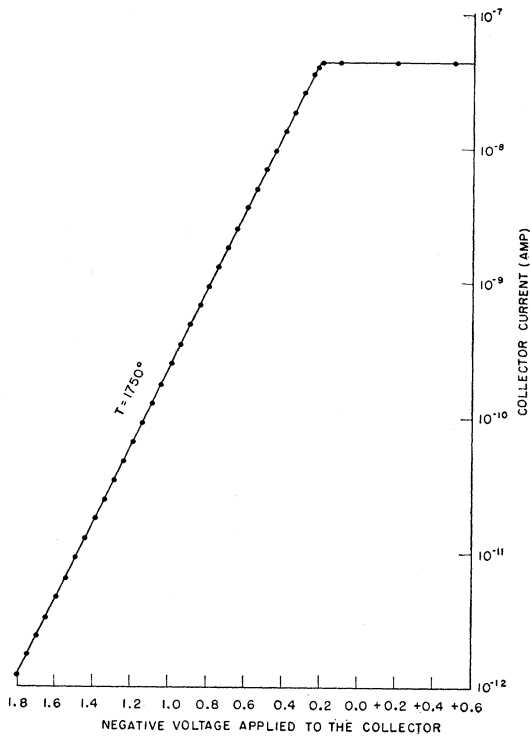


FIG. 2. Retarding-potential plot. The current obeys  $J = J_s \times \exp(-e\Delta V/kT)$  over many orders of magnitude up to the point of complete saturation. The plus signs in the right-hand part of the abscissa refer to positive voltage applied to the collector.

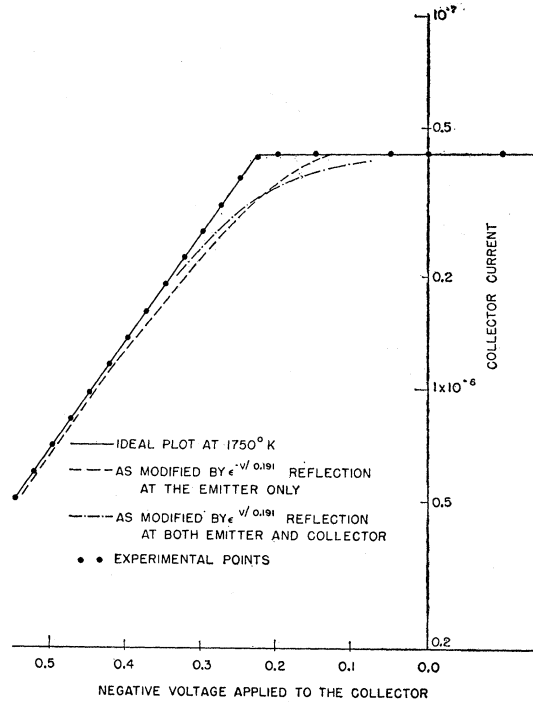


FIG. 3. Expanded knee region of Fig. 2 compared with the theoretical curves with and without the  $\exp(-V/0.191)$  reflection.

plot is shown. It is a straight line on semilogarithmic paper extending to approximately 10 mv of the intersection of the line with the saturated current value. Some curvature of this approximate magnitude is expected from the filament *IR* drop across the emitting region. Equally significant is the flatness of the saturated region. This is rarely seen in retarding-potential experiments, since the accelerating voltage usually manages to collect more current by influencing trajectories, reducing space charge, altering the average potential outside of patchy surfaces, and by other devious means.

Figure 3 shows the upper part of this retarding-potential plot expanded and compared with the calculated currents that would be observed in a retarding-potential experiment if the temperature-dependent reflection of the form  $R = \exp(-V/0.191)$ , as found by Nottingham and Hutson, were present. The agreement of the experimental points with the theoretical curve strongly indicates that this reflection does not exist and, therefore, that it does not influence the experimentally determined value of *A*.

Information concerning a small reflection that has a slow energy dependence can be obtained by observing the collector current as a higher positive voltage is applied. With the potentials applied to the tube, the electrons reflected from the collector with no loss of energy have a negligible chance of returning, while secondary electrons that suffer a loss of a few volts are recollected. The observed increase of collector current with applied voltage, as seen in Fig. 4, can be explained

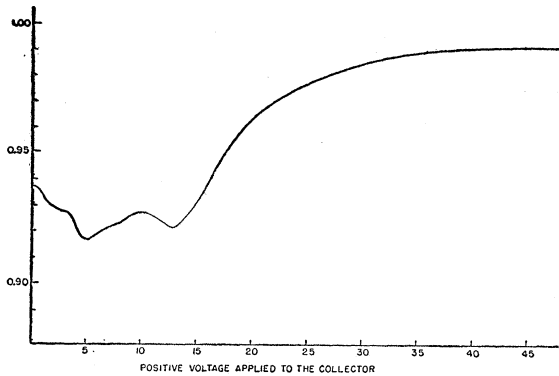


FIG. 4. Transmission of impinging electrons into the collector. This approximate 6% reflection at low energies, which disappears at high energies, agrees with the quantum-mechanical prediction.

as follows: At low energy the approximate 6% reflection results in the collection of less than the impinging current. As more and more positive voltage is applied to the collector, the electrons enter with greater energy and the result is less reflection. This 6% reflection and this energy dependence are predicted by quantum mechanics.<sup>3</sup> The small variation seen at low voltages resembles Bragg reflection, is sensitive to exact surface conditions, and remains unexplained.

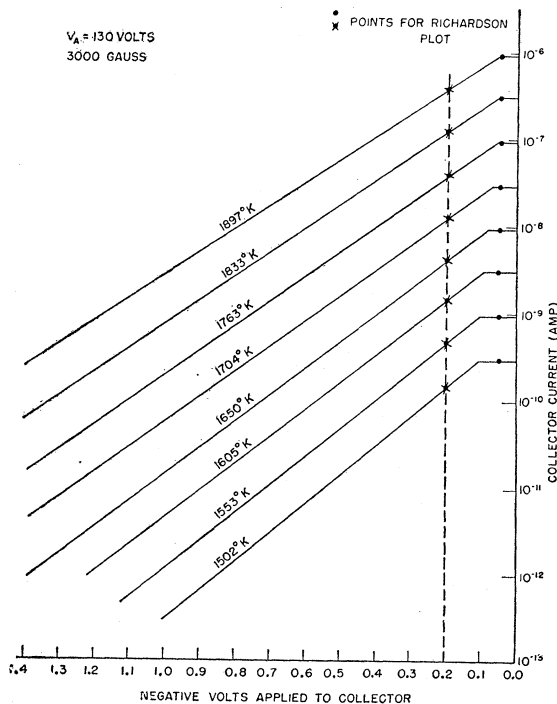


FIG. 5. Typical family of retarding-potential plots from which all information is taken. Temperatures are calculated from the slopes. The temperature derivative of the work-function is seen as a shift of the contact potential. Current densities are just the current divided by the  $1.07 \times 10^{-8} \text{ cm}^2$  area.

<sup>3</sup> C. Herring and M. H. Nichols, *Revs. Modern Phys.* 21, 185 (1949).

The presence of a persistent impurity that would migrate onto the surface of the crystal and form a stable atomic-film emitter allowed the analysis of various surfaces other than the clean, pure-metal surface that was obtained after the impurity was removed by extremely vigorous heat treatment. The method of taking measurements and the analysis of one of these surfaces is illustrated as follows. Figure 5 shows a family of retarding-potential plots taken at different temperatures. The temperature was determined analytically from measured values by averaging the slopes obtained by using measured points about two decades apart. This eliminated the necessity of correcting for

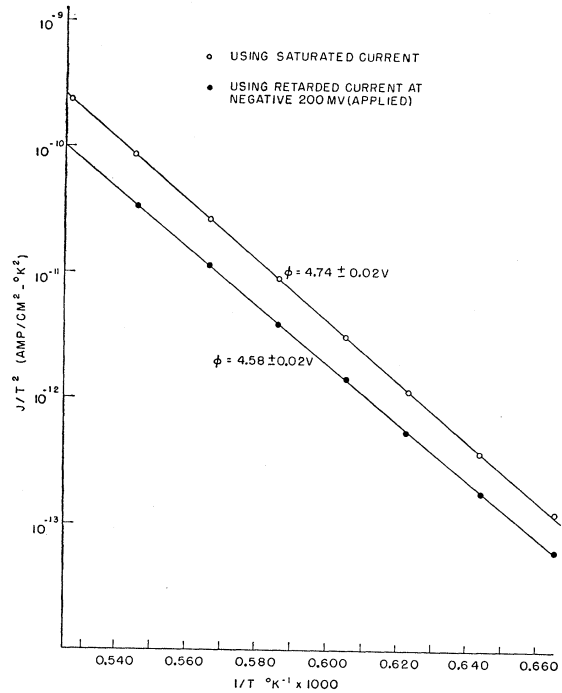


FIG. 6. Richardson plots, based on data from Fig. 5. When saturated current densities are used, an  $A$  value of approximately 1000 results because of  $d\phi/dT$ . Current densities delivered over a temperature-independent barrier that is fixed by the negative collector yield an  $A$  value of 120.

the drop across the microammeter. The currents associated with these temperatures, which are plotted on a Richardson plot, are both the measured values at the fixed applied retarding potential of  $-0.2$  volt, as shown by the crosses, and the saturated current, as shown by dots. The knee of the curves progressively to the right for the higher temperatures, which indicates that the work-function of the emitter is decreasing, and the emission is increasing faster than it would if the work-function remained constant. This is demonstrated in the two Richardson plots shown in Fig. 6. The currents taken at  $0.2$  volt have to go over a barrier that is determined by the collector work-function and the applied voltage. This barrier, which is always higher

than the emitter work-function, is constant during the experiment, and hence the current is unaffected by changes in the emitter work-function. These currents, divided by the area  $1.07 \times 10^{-3} \text{ cm}^2$  to give current density  $J$ , when plotted on a Richardson plot, yield a straight line which gives  $\phi = 4.58 \pm 0.02$  volts and  $A = 130 \pm 25 \text{ amp/cm}^2 \text{ }^\circ\text{K}^2$ . Since we have imposed the condition that  $d\phi/dT = 0$ , these must be the real thermionic constants. When the saturated currents are plotted, however, the apparent work-function is not less—as we know it must be with the smaller barrier—but higher, and it is 4.74 volts. The associated  $A$  is  $950 \text{ amp/cm}^2 \text{ }^\circ\text{K}^2$ . In Fig. 7 the work-function, as calculated by measuring the distance of the knee from  $-0.20$  volt and subtracting it from 4.58 volts, is plotted at the top. The solid line is the best linear representation of the points, neglecting the high-temperature point, which is probably off because of slight space charge. This line gives

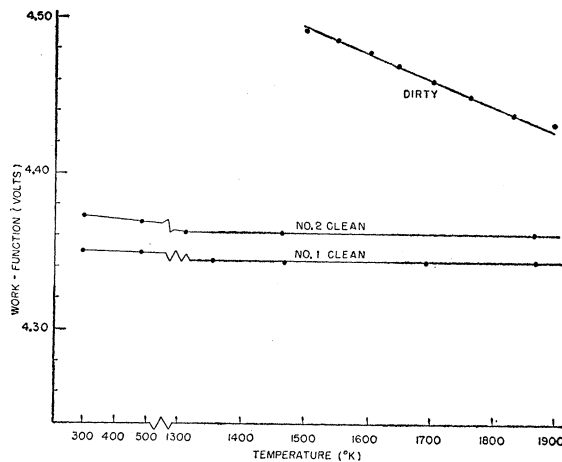


FIG. 7. The work-function of the two clean (211) crystals measured from the highest emitting temperature to room temperature. Also shown is the work-function of the atomic-film emitter which was used as an example.

$d\phi/dT$  equal to  $-0.17 \times 10^{-4}$  volt per degree. Modifying the  $A$  by the factor  $10^{-5040\alpha}$  again yields a true  $A$  of  $130 \text{ amp/cm}^2 \text{ }^\circ\text{K}^2$ . Here is an example of how a simple Richardson plot, in which only the temperature and the saturated current density are used, yields an errone-

ous work-function and  $A$  value, solely because of the temperature variation of the emitter work-function. Similar analyses on all of the composite surfaces that were encountered yielded corrected  $A$  values of approximately  $120 \text{ amp/cm}^2 \text{ }^\circ\text{K}^2$ .

From runs similar to those shown in Fig. 5, but with the exception that a clean filament is used, a Richardson plot was made. The temperature derivative of the work-function was barely detectable; therefore the saturated current density used for the plot should yield the real emission constants. The  $\phi$  came out to be 4.36 volts; the  $A$  value, 110. To extend the measurement of the work-function from the lowest emitting temperature to room temperature, the opposite ribbon was operated as the emitter at a constant high temperature (to mask small currents) while the contact potential was monitored as the temperature of the collector was varied. The temperature derivative of the work-function was detectably negative, but was less than 5 mv in the  $1000^\circ$  range from  $300^\circ\text{K}$  to  $1300^\circ\text{K}$ . This was done with both filaments. The work-function from room temperature up to the highest emitting temperatures is plotted in Fig. 7. Although the two crystals were presumably originally identical, their work-function differed by 15 mv. This disagreement probably results from different effects of the rigorous processing and dc smoothing effects<sup>4</sup> from the heating current. The average work-function is  $4.352 \pm 0.01$  volts with an  $A$  value of  $120 \pm 20 \text{ amp/cm}^2 \text{ }^\circ\text{K}^2$ . Whenever  $d\phi/dT$  is inferred from the shift of the contact potential, a small correction, because of the variable thermal emf of the hot emitter, has to be applied. Conflicting data in published results make the value of this correction unknown. It is reasonably small and was not applied here. Another factor that would make the exact determination of  $A$  differ from 120 would be the known small value of reflection of 6%. However, from the above analysis it is impossible to determine  $A$  to this degree of accuracy.

#### ACKNOWLEDGMENTS

The author is indebted to Professor W. B. Nottingham, under whose supervision this study was initiated and completed.

<sup>4</sup>D. B. Langmuir, *Acta Metallurgica* 5, 13 (1957).